



HAL
open science

Effect of bottom cell properties on micromorph tandem device performance

Paola Delli Veneri, Lucia Vittoria Mercaldo, Carlo Privato

► **To cite this version:**

Paola Delli Veneri, Lucia Vittoria Mercaldo, Carlo Privato. Effect of bottom cell properties on micromorph tandem device performance. *Philosophical Magazine*, 2009, 89 (28-30), pp.2645-2654. 10.1080/14786430902785344 . hal-00519084

HAL Id: hal-00519084

<https://hal.science/hal-00519084>

Submitted on 18 Sep 2010

HAL is a multi-disciplinary open access archive for the deposit and dissemination of scientific research documents, whether they are published or not. The documents may come from teaching and research institutions in France or abroad, or from public or private research centers.

L'archive ouverte pluridisciplinaire **HAL**, est destinée au dépôt et à la diffusion de documents scientifiques de niveau recherche, publiés ou non, émanant des établissements d'enseignement et de recherche français ou étrangers, des laboratoires publics ou privés.



Effect of bottom cell properties on micromorph tandem device performance

Journal:	<i>Philosophical Magazine & Philosophical Magazine Letters</i>
Manuscript ID:	TPHM-08-Sep-0330.R1
Journal Selection:	Philosophical Magazine
Date Submitted by the Author:	12-Jan-2009
Complete List of Authors:	Delli Veneri, Paola; ENEA Meraldo, Lucia; ENEA Privato, Carlo; ENEA
Keywords:	microcrystalline Si:H, thin-film solar cells
Keywords (user supplied):	tandem



Effect of bottom cell properties on micromorph tandem device performance

Paola Delli Veneri^{*}, Lucia V. Mercaldo, Carlo Privato

ENEA - Portici Research Center
Località Granatello, 80055 Portici (Napoli) - Italy

Abstract

Micromorph tandem solar cells represent an elegant way of overcoming the efficiency limits of single-junction solar cells and reducing the light-induced degradation of amorphous silicon films. Micromorph devices have been realized on Asahi U-type TCO-covered glass substrates by very high frequency plasma enhanced chemical vapour deposition (VHF-PECVD) at 100 MHz at low substrate temperature (150 °C). For the bottom cell different growth regimes have been explored by changing both chamber pressure and plasma power aiming at finding interesting regimes for industrial application. The effect of the structural composition of the microcrystalline absorber layer on the electrical parameters of the device has been investigated. The highest efficiency (11.1%) is reached at 67 Pa and power to pressure ratio of 0.3 W/Pa. On the other hand, using larger power to pressure ratio (0.5 W/Pa) high short circuit current density and constant efficiency in a wide silane concentration range are obtained. Homogeneity problems and low response at high wavelengths are found at large pressure (200 Pa). An evaluation of micromorph device stability has also been carried out.

Keywords: Thin Film solar cells, Microcrystalline Si:H, Tandem.

1. Introduction

Micromorph tandem solar cells, stacked structures consisting of a high band gap (1.7 eV) p-i-n amorphous silicon cell on top of a low band gap (1.1 eV) p-i-n microcrystalline silicon cell, have been firstly introduced by IMT Neuchatel [1]. These devices combine the advantages of amorphous silicon and its technology with the stability and spectral sensitivity at long wavelengths of microcrystalline silicon. High efficiencies have indeed been reported by several research groups [1–3] and recent progress in up-scaling has led to production announcements [4–7]. However, since the properties of the microcrystalline material are strongly influenced by the deposition conditions, a deeper understanding of the growth regimes is needed in order to make these devices competitive at industrial level. Moreover, the behaviour of micromorph devices under light soaking is an important issue that needs to be addressed. As a matter of fact, the best microcrystalline cells are deposited around the transition from crystalline to amorphous growth [8], and then both top and bottom cell might in principle contribute to the degradation effect in the overall device.

In this paper our investigation on VHF-PECVD grown micromorph tandem solar cells with different bottom cells is reported. A low deposition temperature (150 °C) has been selected, in order to easily transfer this technology on low cost plastic substrates in a future step. The single cell components have also been analyzed in view of their utilization within the tandem structure. For the microcrystalline bottom cell, two different growth regimes, characterized by two values of plasma power to chamber pressure ratios, have been explored.

^{*} Corresponding Author: Paola Delli Veneri, Tel: +39-081-7723259, fax: +39-081-7723344, e-mail: paola.delliveneri@portici.enea.it

1
2
3
4
5
6
7
8
9
10
11
12
13
14
15
16
17
18
19
20
21
22
23
24
25
26
27
28
29
30
31
32
33
34
35
36
37
38
39
40
41
42
43
44
45
46
47
48
49
50
51
52
53
54
55
56
57
58
59
60

Materials with different structural composition have been taken into account as intrinsic absorber layers, by using different silane concentrations in the gas mixture. An efficiency of 11.1% has been reached, and an interesting regime for industrial application has been evidenced. The devices have also been light-soaked for 200 h and a dependence of the efficiency loss on the crystallinity of the bottom absorber layer has been detected.

2. Experimental

Micromorph tandem solar cells have been deposited on $10 \times 10 \text{ cm}^2$ Asahi U-type TCO-covered glass substrates. The top p-i-n structure consists of a 7 nm thick amorphous silicon-carbide p-layer, a 270 nm thick amorphous silicon i-layer, and a 30 nm thick microcrystalline n-layer. The bottom cell consists of a 30 nm thick microcrystalline p-layer, a 1.5 μm thick microcrystalline i-layer, and a 40 nm thick microcrystalline n-layer. A ZnO back-reflector, followed by 1 cm \times 1 cm Ag pads, has been deposited.

The intrinsic layers of both the amorphous top cell and microcrystalline bottom cell are grown by Very High Frequency Plasma Enhanced Chemical Vapour Deposition (VHF-PECVD) at 100 MHz at low substrate temperature (150 °C). The electrode configuration consists of a $13 \times 13 \text{ cm}^2$ powered electrode and a $11 \times 11 \text{ cm}^2$ substrate carrier as the grounded electrode. The inter-electrode distance is kept at 15 mm, and the gas supply is a simple cross-flow geometry. The plasma power and chamber pressure are kept respectively at 5 W and 27 Pa in the amorphous case, while different growth regimes have been explored in the microcrystalline case. The pressure has been varied from 40 to 200 Pa, and correspondingly the power has been raised from 12 up to 60 W. In particular, two regimes characterized by power to pressure ratio equal to 0.3 W/Pa and 0.5 W/Pa have been selected for investigation. The material has been deposited with different silane concentrations ($\text{SC} = \text{SiH}_4/(\text{SiH}_4+\text{H}_2) = 4.8 - 8.2 \%$) in order to be in the so-called amorphous-to-microcrystalline transition regime [8]. The deposition rate, evaluated from thickness measurements performed by a step profiler, goes from $\sim 3 \text{ \AA}/\text{sec}$ at low pressure (40 and 67 Pa) to $\sim 7-8 \text{ \AA}/\text{sec}$ at 200 Pa.

Doped layers are grown by conventional RF-PECVD technique (13.56 MHz) in a separate chamber of the same cluster-tool deposition system, using phosphine and diborane as dopant gases to prepare n-type and p-type materials respectively. Details about deposition parameters and properties of the doped layers are published elsewhere [9].

Some properties of the single component cells have also been investigated. H_2 -diluted and undiluted amorphous silicon single junctions ($\text{H}_2/\text{SiH}_4=0,2,9$) have firstly been fabricated in order to study the effect of different band gaps on the J-V characteristic. Transmission measurements, using a Perkin Elmer λ -900 spectrophotometer, have also been performed on intrinsic amorphous silicon thin films in order to measure the parameter E_{04} (energy value corresponding to $\alpha = 10^4 \text{ cm}^{-1}$). Microcrystalline p-i-n single junctions with different p-layers have been fabricated: in particular two values of hydrogen dilution, $\text{H}_2/(\text{H}_2+\text{SiH}_4) = 99\%$ and 99.3%, have been selected. The 1 μm thick absorber layer has been deposited in the same conditions (67 Pa, 20 W, and $\text{SC} = 5.2\%$).

The devices have been characterized by measuring spectral response and current-voltage J(V) characteristic under AM1.5 illumination. Variable Intensity Measurements (VIM), i.e. J(V) curves at $0.01-100 \text{ mW}/\text{cm}^2$, have been made in order to evaluate the shunt resistance [10]. The light-soaking has been carried out at open circuit under an AM 1.5 solar simulator for 200 hours at 30 °C. We have also probed the crystallinity of the devices by determining the Raman spectra with the strongly absorbed 514 nm line of an Ar^+ laser and/or the weakly absorbed 633 nm line of a HeNe laser. We have evaluated crystalline and amorphous phase

fraction as $\Phi_c = (I_{520} + I_{510}) / (I_{520} + I_{510} + I_{480})$ and $\Phi_a = I_{480} / (I_{520} + I_{510} + I_{480})$ respectively, where I_i is the area under the peak centered at wavenumber i [11].

3. Results and discussions

3.1 Single component cells

When fabricating a micromorph tandem solar cell, the basic problem is combining a high-current but low-voltage microcrystalline cell with a low-current but high-voltage amorphous cell. We firstly focused on the amorphous top cell. It is known that amorphous silicon deposited with hydrogen dilution have enhanced stability against light soaking [12]. However hydrogen dilution reduces the optical absorption, and this turns out in lower current densities [13].

We have included different types of amorphous material as absorber layer in single p-i-n junctions, in order to evaluate the effect of different band gaps on the J-V characteristic. In Table I we report the E_{04} values determined by transmission experiments on films deposited with different hydrogen to silane flow ratios in the gas mixture. The higher optical gap of the H_2 -diluted material translates into larger open circuit voltage, but lower short circuit current, as shown in the same table. In order to enhance the efficiency of micromorph tandem cells the optical absorption in the top cell must be increased. As a matter of fact, due to the high current potential of the microcrystalline bottom cell, it is preferable to optimise the top cell in order to obtain a high current rather than a high voltage. Therefore, as already done elsewhere [13], undiluted amorphous silicon has been chosen to be inserted in the top cell of the tandem devices. In our case, however, the absorber material is grown at lower substrate temperature (150 °C), which still allows for a sufficiently high short circuit current density.

Moreover, for both the single component cells special attention must be paid on the p-layer. Since optical absorption within the p-layer can limit J_{SC} , material with wide optical gap is desired. At the same time, this layer has to be highly conducting and, for microcrystalline p-i-n solar cells, sufficiently crystalline to promote the nucleation of the superimposed microcrystalline i layer at the p/i interface [14].

However, too large crystalline phase fraction could also be deleterious, as illustrated in Table 2. Here structural and electrical parameters of two microcrystalline p-i-n solar cells with different p-layers, grown with two different values of hydrogen dilution, are reported. The crystalline phase fraction Φ_C in Table 2 has been evaluated through Raman analysis, with focused Ar^+ laser (514 nm) arriving through the glass substrate and the TCO (transparent conducting oxide) on the first-deposited silicon p-layer of the device. The collected Raman contribution arises from the doped layer (about 25 nm) and the first tens of nanometers of the i-layer [11]. The overall device performance is worse for the cell that includes a more crystalline p-layer (M-P2), and the quantum efficiency (Fig. 1) shows a clear loss in the low wavelength range (360-600 nm) for this device.

By using the Variable Illumination Measurement technique (VIM) [10] at very low illumination levels, lower shunt resistance (R_{Sh}) has been evaluated on device M-P2 ($3 \text{ k}\Omega\text{-cm}^2$) (Table 2). Then, a possible correlation between large crystalline phase fraction in the p-layer and formation of cracks can be advanced. The presence of cracks through the p-layer and the first part of the absorber layer close to the p/i interface could explain the reduced spectral response and the lower V_{OC} . Moreover, the presence of cracks could favour boron diffusion and give rise to a thicker effective p-layer which would contribute to the reduced quantum efficiency in the blue-green wavelength range.

1
2
3
4
5 Summarizing, undiluted amorphous silicon deposited at low temperature (150°C) is
6 selected as absorber layer for the top cell. The window p-layers need special care: in
7 particular for the microcrystalline component cell a crystalline phase fraction for such doped
8 layer around 60% has been chosen to avoid possible formation of cracks at the interface with
9 the i-layer.
10

11 12 13 *3.2 Tandem devices*

14
15 For each pressure value a series of tandem cells has been fabricated with the intrinsic layer in
16 the bottom cell grown with different silane concentration values, in order to study the effect of
17 the structural composition on the device performance and find the optimum phase mixture.
18 Such material, which results in the highest solar cell efficiency, is found within the transition
19 region from crystalline to amorphous growth [8]. The thickness of the active layers has been
20 fixed to 270 nm for the top cell and 1.5 μm for the bottom cell. In all cases the fabrication
21 conditions for the top cell have never been changed, therefore all the variations observed in
22 the photovoltaic parameters are due to the bottom cell. Table 3 shows the main deposition
23 parameters of the bottom absorber layer of the five series discussed in the paper, realized by
24 using a power to pressure ratio equal to 0.3 W/Pa (series name ending with A) or 0.5 W/Pa
25 (series name ending with B).
26

27
28 The electrical parameters extracted from the J-V characteristics of the cells are shown in
29 figure 2. The amorphous to crystalline transition region is determined by all the deposition
30 parameters, therefore the relative positions of all the curves along the SC axis is not always
31 significant. In all cases FF, J_{SC} and the efficiency first increase with silane concentration and
32 then drop after reaching their maximum values, while V_{OC} monotonously increases with SC
33 and is approximately equal to the sum of the V_{OC} values of the single cells [Table 1 and 11],
34 thus evidencing negligible losses at the tunnel recombination junction.
35

36
37 Looking at the A-type series first (solid symbols in the figure), pronounced peaks for J_{SC} ,
38 FF and η have been obtained. The maximum J_{SC} values are almost the same in all cases
39 (11.6–11.8 mA/cm^2). However an overall improvement is registered when the pressure is
40 raised from 40 to 67 Pa, while at much larger pressure (200 Pa - series T200A) a general
41 deterioration of all the parameters is found. The worse electrical parameters found for series
42 T40A could be related to the low power (12 W), maybe not sufficient to grow a good quality
43 microcrystalline material with low defect density. Poor quality of the bottom absorber
44 material can be expected also in the high pressure regime, due to the larger growth rate. As a
45 matter of fact quantum efficiency measurements on the bottom cell of devices from series
46 T200A show a low response for the red and near-infrared wavelengths, as already reported in
47 literature [15]. Moreover, at 200 Pa some difference in the performance among the devices
48 realized on the $10 \times 10 \text{ cm}^2$ substrate, excluding the cells positioned in the central part of the
49 substrate, is present due to structural and thickness inhomogeneity. For all these reasons no B-
50 type series has been realized at high pressure.
51

52
53 Both the B-type series (open symbols in the figure) have large current values and almost
54 constant FF and η in a wide SC range. However, lower V_{OC} values have been obtained with
55 respect to the A-type series, due to the worse p/i interface when high power to pressure ratio
56 is used to grow the bottom absorber material. The lowest V_{OC} values have been found for
57 series T67B thus giving indication of further worsening of the p/i interface when high power
58 is used.
59

60
The main difference among A- and B-type series resides in the wideness of the amorphous
to crystalline phase transition region, as confirmed by Raman analysis. In Fig. 3 the spectra
obtained with focused excitation light (633 nm) arriving on the last-deposited silicon n-layer

1
2
3
4
5
6
7
8
9
10
11
12
13
14
15
16
17
18
19
20
21
22
23
24
25
26
27
28
29
30
31
32
33
34
35
36
37
38
39
40
41
42
43
44
45
46
47
48
49
50
51
52
53
54
55
56
57
58
59
60

are shown for the two series deposited at 67Pa and different power levels. In this case the collected Raman contribution arises from the doped layer (about 40 nm) and about half of the microcrystalline i-layer [11], and then it gives a good indication of the crystallinity of the bottom absorber layer. For series T67B (Fig. 3(b)) the crystalline phase fraction is practically the same in a wide SC range (5.2-7.4%), whereas in the same range a rapid variation of crystalline phase fraction is observed for series T67A (Fig. 3(a)). In this last case Raman analysis reveals a mixed material ($\Phi_a = 48\%$) at SC = 5.5% and an almost totally amorphous material at SC = 7.2%. Moreover generally larger crystalline phase fractions are registered in the B-type series.

A peculiar behaviour of series T40B ought to be pointed out, namely the large short circuit current density (up to 12.4 mA/cm² at SC = 5.4%) even if Raman analysis reveals a narrower transition region when compared to series T67B. In particular, the large current densities measured in this case are obtained with bottom absorber materials characterized by crystallinity values between 36% and 64%. This means that even with relatively low crystalline phase fractions it is possible to generate/collect large currents. Since this series has the same doped layers and back reflector as the others, we do not expect enhanced light scattering at the back reflector or improved efficiency of carrier collection. Therefore, these larger currents can be explained by means of a bulk material with a structure particularly apt to scatter the impinging radiation within the device and then optimize the absorption and carrier generation [16]. This assumption finds a confirmation in the spectral response of the cells of series T40B. In Fig. 4 we show the quantum yield of the best cell of series T40B (SC = 5.9%) and T67A (SC = 6.1%). As expected no change is observed for the top cell, whereas the bottom cell from series T40B shows a larger response for the red and near-infrared wavelengths, which can be interpreted in terms of a better absorption of the radiation within the bottom microcrystalline i-layer.

The large currents measured on series T40B are not accompanied by sufficiently high V_{OC} values. In the micromorph structure, due to the low current of the top cell, it is preferable, within some limits, to choose an absorber material for the bottom cell that furnishes a high voltage rather than a high current. Therefore, the efficiency is maximized within series T67A (11.1%), where generally larger V_{OC} values are obtained, coupled with FF > 70%. However, we want to point out that such growth regime is characterized by a more pronounced dependence on SC. The weak dependence of J_{SC} , FF and η on silane concentration found when using high power to pressure ratio (0.5 W/Pa), makes this condition very interesting for industrial application, where a precise control of gas concentration on large areas can be difficult.

Finally, the stability of the micromorph devices has been evaluated by exposing the cells to white light for 200 hours, a sufficiently long time to extract meaningful indications on the light-soaked state, even if saturation is not yet reached. As expected, lower relative efficiency loss, $\Delta\eta = (\eta_{initial} - \eta_{degraded}) / \eta_{initial}$, is found when Φ_C in the bottom cell is larger, due to the stability of the crystalline phase. Generally, $\Delta\eta$ ranges in between 5 and 9%, depending on Φ_C . Larger efficiency losses ($\Delta\eta \sim 13\%$) have been registered only for the devices from series T40B grown at low SC that appear top cell (more unstable) limited devices from QE measurements. In fact, the opposite condition, with the more stable component cell limiting the output current, was already shown to significantly improve the stability of tandem devices [17]. We can conclude that, due to the better stability of the microcrystalline component cell, a bottom cell limited current mismatch is preferable in micromorph devices in order to contain the light-induced degradation effect. In this condition the best devices have $\Delta\eta < 6\%$.

4. Conclusions

Micromorph tandem solar cells have been fabricated by VHF-PECVD at 100 MHz at low deposition temperature (150°C). Undiluted amorphous silicon has been chosen as the optimal absorber layer for the top cell, because of its lower band gap, allowing for larger currents. An optimal crystallinity for the p-layer within the microcrystalline component cell has been evaluated around 60%, to avoid possible formation of cracks at the interface with the i-layer, evidenced with larger crystalline phase fraction. Different deposition regimes for the bottom cell within the micromorph device have been investigated. The power to pressure ratio has been identified as an important parameter. The best performance, with an initial efficiency of 11.1%, has been found at low power to pressure ratio (0.3 W/Pa), when growing the bottom absorber layer at 67 Pa, due to the larger V_{OC} and FF values obtained in this regime. At much larger pressure (200 Pa), where interestingly high deposition rates ($\sim 7 - 8 \text{ \AA/s}$) are obtained, absorber material with low response at red and near-infrared wavelengths is grown and some homogeneity problems are evidenced on the $10 \times 10 \text{ cm}^2$ substrate area. In the large power to pressure ratio regime (0.5 W/Pa), devices with high short circuit current density and constant FF in a wide SC range are obtained. In particular, a J_{SC} of 12.4 mA/cm^2 has been reached at 40 Pa. The weak dependence of J_{SC} , FF and η on silane concentration makes this regime very interesting for industrial application, where the production of large area devices asks for non-trivial control of gas-distribution uniformity. Finally, light-soaking of the tandem solar cells has shown that the efficiency loss depends on the crystallinity of the bottom absorber layer, and devices with a bottom cell limited current mismatch are preferable in order to maintain high efficiency in the degraded state. In this condition, after 200 hours an efficiency loss lower than 6% has been measured on the best solar cells.

References

- [1] J. Meier et al. Proc. first WCPEC, Hawaii, USA, 1994 p.409.
- [2] J. Meier et al., Sol. Energy Mater. Sol. Cells 74 (2002) p.457.
- [3] K. Yamamoto et al., Sol. Energy Mater. Sol. Cells 74 (2002) p.449.
- [4] M. Yoshimi et al., Conference Record, 3rd World Conference on Photovoltaic Energy Conversion, Osaka, May 2003, p.1566.
- [5] U. Kroll et al., Proceedings of 22st European Photovoltaic Solar Energy Conference, Milan, Italy, 3-7 September 2007, p.1795.
- [6] Y. Chae et al., Proceedings of 22st European Photovoltaic Solar Energy Conference, Milan, Italy, 3-7 September 2007, p.1807.
- [7] H. Takatsuka, Proceedings of 21st European Photovoltaic Solar Energy Conference, Dresden, Germany, 4-8 September 2006, p.1531.
- [8] O. Vetterl et al., Sol. Energy Mater. Sol. Cells 62 (2000) p.97.
- [9] P. Delli Veneri, L.V. Mercaldo, C. Minarini, C. Privato, Thin Solid Films 451-452 (2004) p.269.
- [10] J. Merten et al, IEEE Transactions on electronic devices 45 (1998) p.423.
- [11] P. Delli Veneri, L. V. Mercaldo, P. Tassini, C. Privato, Thin Solid Films 487 (2005) p.174.
- [12] S. Guha, K.L. Narasimhan, S.M. Pietruszko, J Appl Phys 52 (1981) p.859.
- [13] R. Platz, C. Hof, D. Fischer, J. Meier, A. Shah, Sol Energy Mater Sol Cells 53 (1998) p.1.
- [14] S. Hamma, P. Roca i Cabarrocas, Sol. Energy Mater. Sol. Cells 69 (2001) p.217.
- [15] U.S. Graf, J. Meier, A. Shah, Proc. Third World Conference on Photovoltaic Energy Conversion, 2004, p.1663.

[16] Poruba et al., J. Appl. Phys. 88 (2000) p.148.

[17] B. Yan, G. Yue, J. Yang, A. Banerjee, S. Guha, Mater. Res. Soc. Symp. Proc., 762 (2003) p.309.

For Peer Review Only

1
2
3
4
5
6
7
8
9
10
11
12
13
14
15
16
17
18
19
20
21
22
23
24
25
26
27
28
29
30
31
32
33
34
35
36
37
38
39
40
41
42
43
44
45
46
47
48
49
50
51
52
53
54
55
56
57
58
59
60

1
2
3
4
5
6 Table 1 *Left hand side*: Hydrogen to silane flow ratio and optical gap (expressed as E_{04}) for
7 one undiluted and two H_2 -diluted amorphous silicon samples. *Right hand side*: Open circuit
8 voltage and short circuit current density of three amorphous p-i-n solar cells characterized by
9 three different absorber layers described in the left hand side of the table.
10

<i>Amorphous i-layers</i>		<i>Solar cells</i>	
H_2/SiH_4	E_{04} (eV)	V_{OC} (mV)	J_{SC} (mA/cm ²)
0	1.92	860	13.8
2	1.95	870	13.1
9	1.98	885	11.1

Table 2 Structural and electrical parameters of p-i-n microcrystalline solar cells with p-doped layers grown with two different hydrogen dilutions.

	$H_2/(H_2+SiH_4)$ (%)	Φ_C (%)	FF (%)	V_{OC} (mV)	J_{SC} (mA/cm ²)	R_{Sh} (k Ω ·cm ²)
M-P1	99.0	60	62.0	486	20.1	6
M-P2	99.3	68	61.7	475	19.2	3

Table 3 Chamber pressure, plasma power and silane concentration (SC) range used to deposit the series of tandem devices.

Series	Pressure (Pa)	Power (W)	Power/pressure (W/Pa)	SC (%)
T40A	40	12	0.3	5.5 - 7.0
T67A	67	20	0.3	5.5 - 7.2
T200A	200	60	0.3	5.5 - 6.7
T40B	40	20	0.5	4.8 - 8.0
T67B	67	33	0.5	5.2 - 8.2

LIST OF FIGURE CAPTIONS

Fig. 1 Spectral response of the microcrystalline p-i-n solar cells with the p-doped layers described in Table 2.

Fig. 2 Electrical parameters extracted from the J-V characteristics under AM1.5 illumination of the five silane concentration series of tandem cells described in Table 3. Solid and open symbols refer to series grown at power to pressure values of 0.3 W/Pa and 0.5 W/Pa respectively. The lines are guides to the eye.

Fig. 3 Normalized Raman spectra of tandem solar cells from series T67A (a) and T67B (b) obtained with the weakly absorbed 633 nm excitation light arriving on the last deposited n-layer. The amorphous phase fraction Φ_a is also reported in the figures.

Fig. 4 Spectral response of the best micromorph tandem devices from series T40B and T67A.

1
2
3
4
5
6
7
8
9
10
11
12
13
14
15
16
17
18
19
20
21
22
23
24
25
26
27
28
29
30
31
32
33
34
35
36
37
38
39
40
41
42
43
44
45
46
47
48
49
50
51
52
53
54
55
56
57
58
59
60

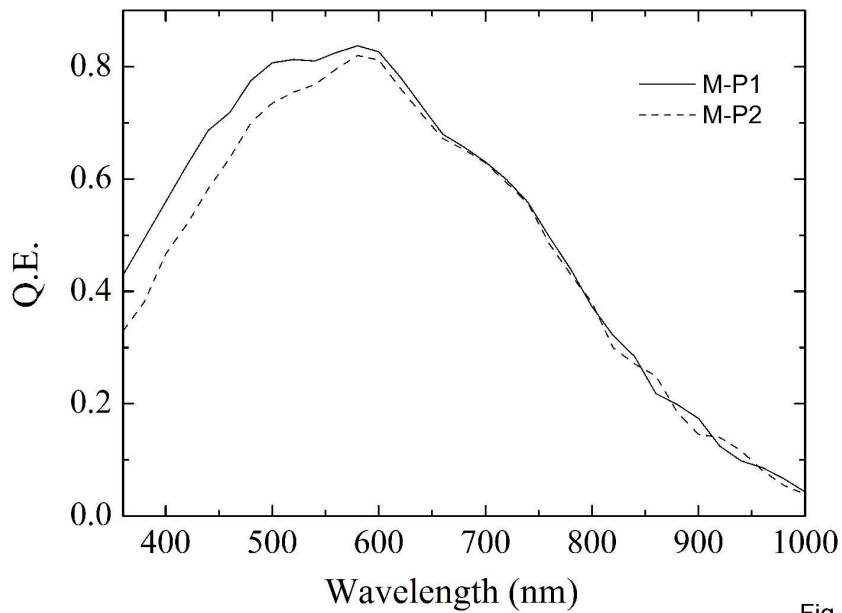


Fig.1

2387x1678mm (72 x 72 DPI)

view Only

1
2
3
4
5
6
7
8
9
10
11
12
13
14
15
16
17
18
19
20
21
22
23
24
25
26
27
28
29
30
31
32
33
34
35
36
37
38
39
40
41
42
43
44
45
46
47
48
49
50
51
52
53
54
55
56
57
58
59
60

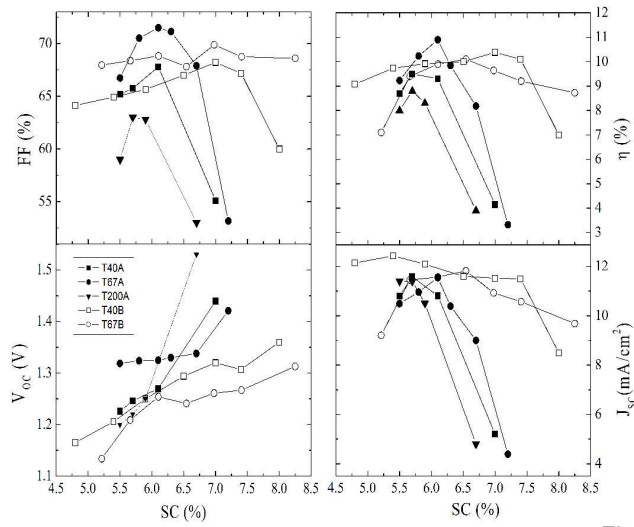


Fig. 2

2390x1678mm (72 x 72 DPI)

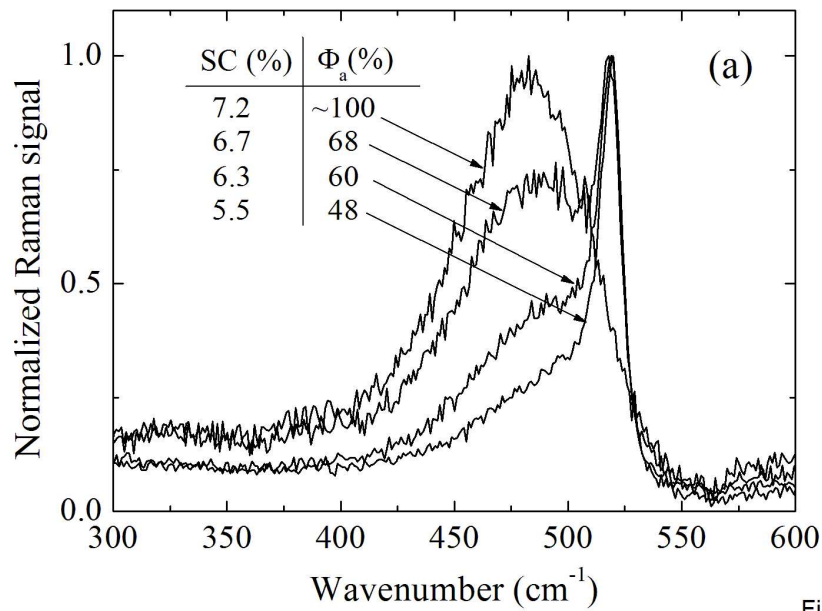


Fig. 3a

599x418mm (72 x 72 DPI)

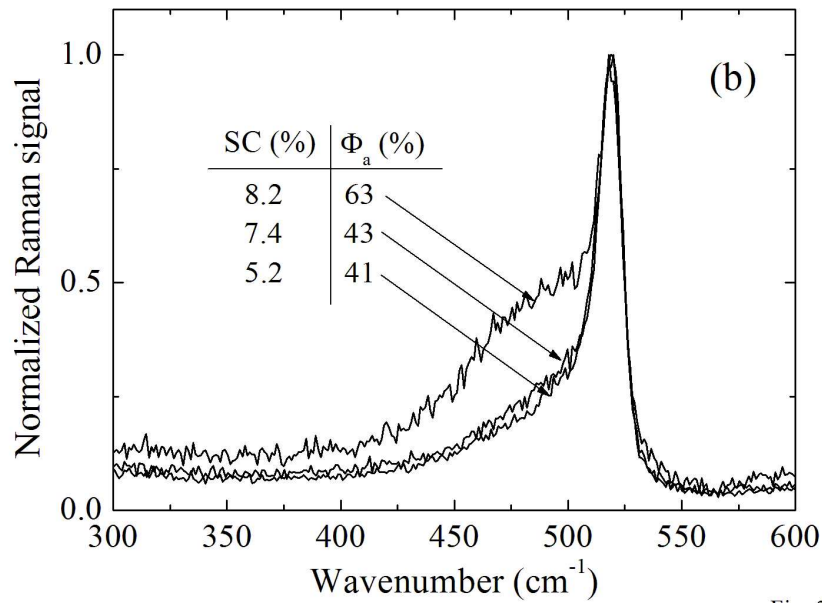


Fig. 3b

599x418mm (72 x 72 DPI)

View Only

1
2
3
4
5
6
7
8
9
10
11
12
13
14
15
16
17
18
19
20
21
22
23
24
25
26
27
28
29
30
31
32
33
34
35
36
37
38
39
40
41
42
43
44
45
46
47
48
49
50
51
52
53
54
55
56
57
58
59
60

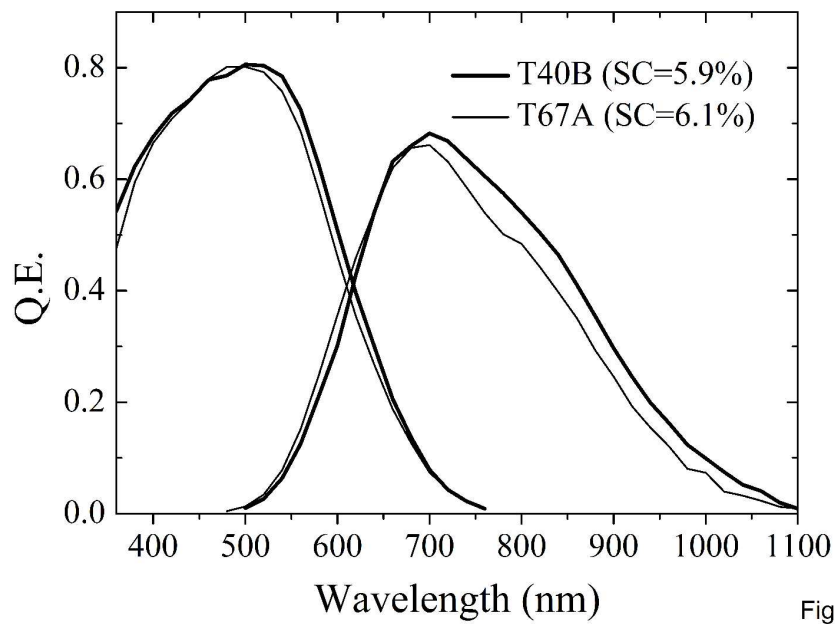


Fig.4

2396x1671mm (72 x 72 DPI)